International Conference on Applied Energy 2019
Aug 12-15, 2019, Västerås, Sweden
Paper ID: 382

MULTI-SCALE EXPERIMENTAL INVESTIGATION ON THE KINETIC BEHAVIOUR OF CH_4-HYDRATE IN SANDY MEDIA

Zhenyuan Yin[1,2], Li Huang [3,4], Praveen Linga [1*]

[1]Department of Chemical and Biomolecular Engineering, National University of Singapore, Singapore, 117582
[2]Lloyd's Register Singapore Pte. Ltd., Singapore, 138522
[3]The Key Laboratory of Gas Hydrate, Ministry of Natural Resources, Qingdao Institute of Marine Geology, Qingdao, China, 266071
[4]Laboratory for Marine Mineral Resources, Qingdao National Laboratory for Marine Science and Technology, Qingdao, China, 266071

ABSTRACT

Two high-pressure reactors with effective volumes of 1.0 L and 3.3 L were employed to investigate the dynamic behavior of methane hydrate formation and dissociation induced by depressurization with the aim of elucidating the difference in production behavior and developing the scaling criteria. Based on the experimental results, to synthesize aqueous-rich MHBS of the same saturations, the amount of hydrate-formers and the sandy media should strictly adhere to the volume ratio. Increasing the sample size of MHBS resulted in 20.7% increase in gas recover ratio and 53.8% decrease in water recovery ratio under bottom hole pressure of 4.0 MPa. Heat transfer direction were similar from outer boundary inward to the core center. Understanding the effect of scaling on production profile could shed light on better experimental design and possibly field production tests.

Keywords: Methane hydrate; Hydrate-bearing sediments; Energy recovery; Production behavior; Depressurization; Scaling analysis

NONMENCLATURE

Abbreviations	
MHBS	Methane hydrate-bearing sediments
BHP	Bottom-hole pressure
Symbols	
$S_{i = A, G, H}$	Saturation of the i^{th} phase
$n_{i = A, G, H}$	Number of mole of the i^{th} phase
$\rho_{i = A, G, H}$	Density of the i^{th} phase
V	Volume
P	Pressure
V_G	Cumulative production of gas
M_W	Cumulative production of water
$t_{50,H}$	Dissociation time for 50% the MH
X_{gas}	Conversion of CH_4 to MH

1. INTRODUCTION

Methane hydrates (MHs) has been considered as the future energy resource because of its large resource volume and its capability to store CH_4 effectively [1]. To recover CH_4 effectively and safely requires a fundamental understanding on the physical behavior of hydrate formation, dissociation and the associated fluid flow in sandy media [2, 3]. However, due to the limited number of hydrate cores extracted from field and the lack of prior knowledge on the HBS, to synthesize artificial hydrate-bearing sediments in laboratory to examine their formation and dissociation behavior and the thermophysical properties is necessary [4].

One common issue often encountered is the difference in temporal and spatial scales between the hydrate reservoir and reactor [5]. Formation of MHBS in laboratory reactor (volume of liters) typically takes tens of days with an effective cooling boundary [6], while formation of MHBS in reservoir could take tens of years with no or not-effective cooling boundary. Similarly, dissociation of MHBS in laboratory are subject to high-temperature or ambient-temperature boundary in laboratory, while dissociation of MHBS in reservoir does not have such boundary effect [7]. Thus, significant doubts are casted on the applicability of laboratory data to the real field production tests [8].

In view of the knowledge gaps identified above [9], we conducted a multi-scale investigation on the dynamic behavior of MHBS using two reactors of different sizes: a V = 3.3 L reactor and a V = 1.0 L reactor. We designed experiments to form aqueous-rich MHBS (S_H = 40% and

Selection and peer-review under responsibility of the scientific committee of the 11th Int. Conf. on Applied Energy (ICAE2019).

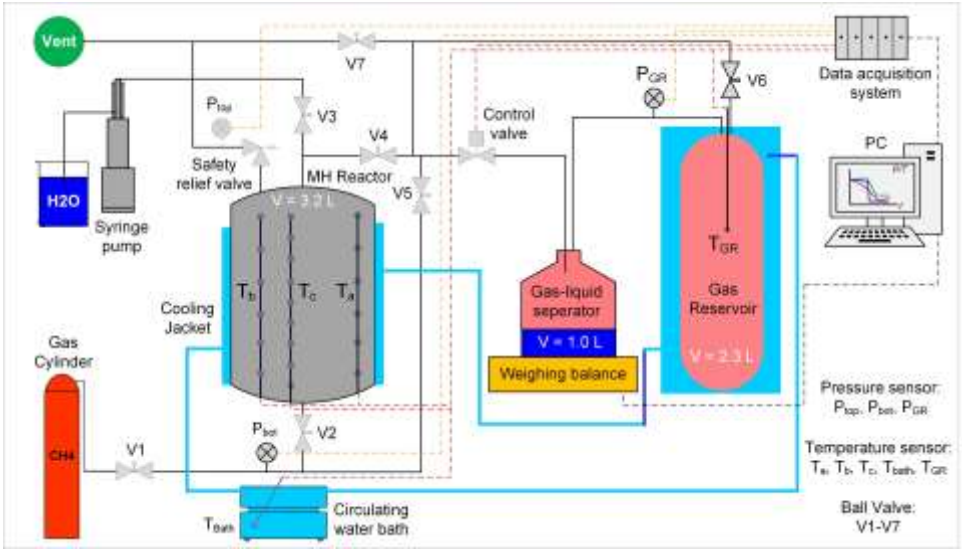

Fig 1. Schematic of the V = 3.3 L hydrate reactor and the fluid production system.

S_A = 60%) with low gas saturation in both reactors and subject the samples to dissociation by depressurization under various bottom hole pressures, BHPs. The objective is to elucidate the effect of scaling on the dynamic behavior of MH formation, dissociation and fluid production in sandy media. By quantifying the phase saturations and fluid production over time, we want to identify the controlling factors in formation and dissociation in the scaled-up apparatus, and possibly develop the scaling criteria for fluid production.

2. EXPERIMENTAL SECTION

2.1 Experimental setup

The experimental apparatus for the V = 1.0 L hydrate reactor has been discussed in detail in our previous paper [10]. Here, we focus our discussion on the new experimental setup, the V = 3.3 L hydrate reactor. The maximum working pressure of the stainless steel reactor is 10.0 MPa. A fluid collection system, which includes a gas-liquid separator (V = 1.0 L) connecting with a gas reservoir (V = 2.3 L) were located downstream of the reactor. A syringe pump (V = 0.5 L) was used for water injection from the top nozzle and the gas cylinder was employed for gas injection from the bottom nozzle. The temperature of the reactor and the gas reservoir was controlled by a circulating water bath.

Two pressure sensors were installed to measure the pressure at the top (P_{top}) and bottom (P_{bot}) location of the reactor with another pressure sensor measuring the gas reservoir (P_{GR}). Three sets of multi-point thermocouple (T_a, T_b, and T_c) were installed inside the reactor to acquire temperature at different radial and vertical locations with another two thermocouples measuring the temperature of the gas reservoir (T_{GR}) and the circulating water bath (T_{bath}). Fig. 2 shows the cross-section view of the reactor and the location of the 21 thermocouple positions. All the P and T data were recorded by a data acquisition system using a user-defined frequency.

2.2 Material

Fine quartz sand with mean diameter, D_{50} = 0.2 mm was used as the sandy medium to form MHBS. The porosity was measured to be 0.44 with permeability as 3.8 Darcys. In addition, pure CH_4 (>99.9%) gas and deionized water were used for MH formation.

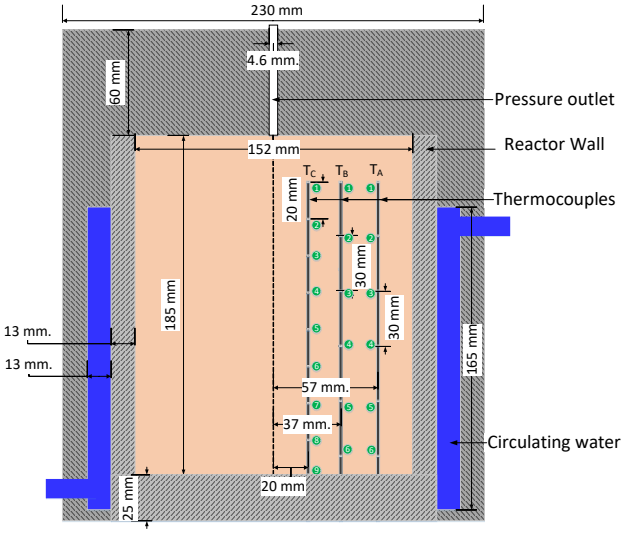

Fig 2. Cross-section view of the V = 3.3 L reactor with dimensions and positions of thermocouples.

2.3 Experimental Procedure

The method to synthesize the aqueous-rich MHBS with S_H = 0.4 and S_A = 0.6 using the excess-water technique has been detailed discussed in our earlier

papers. The key factor is to inject more than the stoichiometric-based water to consume all the free gas in the pore space and to create an aqueous-rich environment.

The MH formation process involves 9 steps in total: (1) air removal, (2) gas injection, (3) 1st water injection, (4) stabilization, (5) 1st MH formation, (6) 2nd water injection, (7) 2nd MH formation, (8) 3rd water injection and (9) 3rd MH formation. Water was injected at a constant flow rate of 30 ml/min in every injection step. Temperature of the reactor was controlled at constant T = 1.0 °C throughout the MH formation period. MH formation was deemed to complete when the pressure drop rate was discernable ($\Delta P/\Delta t$ < 10 kPa/hr).

To prepare the MHBS for dissociation, temperature of the sample was first increased within the MH stable region to T = 6.0 °C, which corresponds to ~150 m below seafloor [11]. The final pressure of the MHBS was ~6.0 MPa, Depressurization was initiated by crack open V4 and the rate of depressurization (i.e the opening of the valve) was controlled by the control valve with a PID controller.

2.4 Method of calculation

To estimate the phase saturation, a pore-volume balance method was employed [12]. The governing equations for the pore volume balance method are listed in Table 1. By solving the coupled non-linear equations based on the measured P and T at each time point, X_G and the corresponding phase saturations can be estimated. Peng-Robinson EOS [13] was used to estimate the compressibility of CH_4 and the solubility of CH_4 in H_2O [14] was accounted to yield a more accurate estimation on S_H.

Table 1: List of governing equations in the pore-volume balance method.

$CH_4+N_HH_2O = CH_4 \cdot N_HH_2O$ (N_H = 6.0)	
Governing Eqn: $V_{pore} = V_G + V_A = V_G + V_A + V_{MH}$	
$V_G = \rho_G \times (n_G - n_G \times X_G - V_A \times S_G)$	ρ_G , $S_G = fn$ (P, T)
$V_A = \rho_A \times (n_A - N_H \times n_G \times X_G)$	ρ_A= 1.0 g/cm^3
$V_{MH} = \rho_{MH} \times n_G \times X_G$	ρ_{MH}= 0.92 g/cm^3

3. RESULTS AND DISCUSSION

3.1 MH formation and dissociation

Fig. 3 presents the trajectory of P_{avg}-T_{avg} during the entire MH formation and dissociation processes in the V = 3.3 L reactor in relation to the CH_4-hydrate equilibrium curve. The formation process (A→K) yielded a complicated trajectory of P-T, especially within the hydrate stability region because of the injections of abundant water into the system to assist MH formation and to create the aqueous-rich environment. The dissociation process (K→L) reflected a typical depressurization technique for MH dissociation.

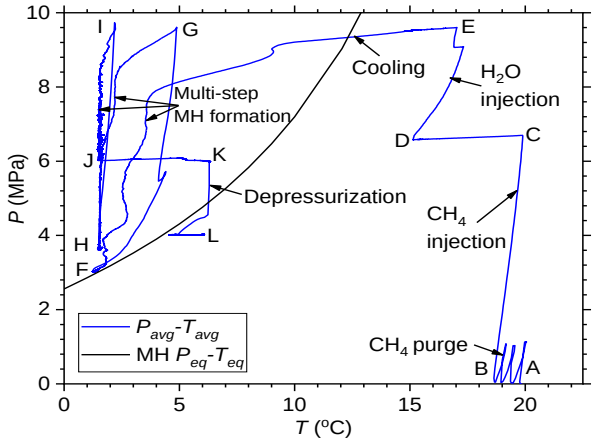

Fig. 3. Trajectory of P_{avg}-T_{avg} during MH formation and dissociation in the V = 3.3 L reactor.

Fig. 4 shows the evolution of P_{avg} and T_{avg} during the entire MH formation process in the V = 3.3 L reactor. The MH formation process took ~150 hr and resulted a final P = 6.0 MPa and T = 6.0 MPa. It is noticed that the three water injection steps resulted in significant increase in P to 9.6 MPa during each stage followed by subsequent hydrate formation. Temperature spikes were observed during the cooling stage because of the exothermic nature of MH formation and also during the water injection stage due to the higher T of the injected temperature. Based on the pore-volume balance method, the final phase saturations are: S_H = 40.4%, S_A = 57.6% and S_G = 2.0% with X_G = 95.2%.

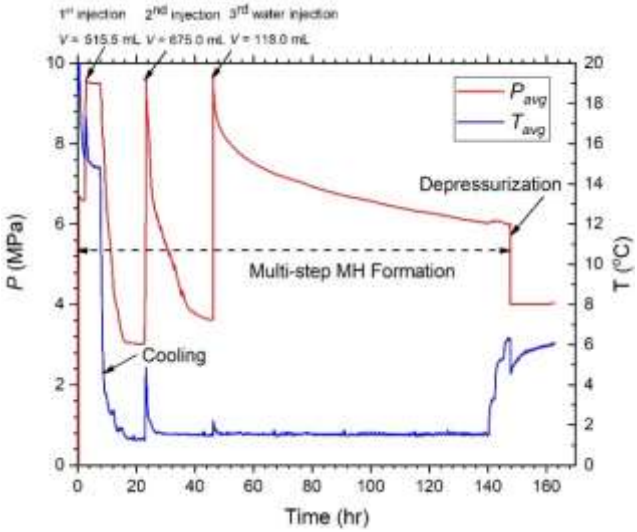

Fig. 4. Evolution of experimental measured P_{avg} and T_{avg} over time during MH formation and dissociation.

3.2 Fluid Production Behavior

Fig. 5 shows the evolution of BHP, V_G and M_W over time during the MH dissociation process induced by a constant BHP. It is observed that BHP decreased step-wise decrease from P = 6.0 MPa to 4.0 MPa within ~100 seconds and maintained constant. The production of V_G showed a continuous increase during the MH dissociation period and reached its final level V_G = 77.2 L after ~16 hrs. The final recovery of gas, R_G attained was 75.7%. The production of M_W showed a step-wise increase pattern instead of continuous and plateaued to a final mass of 263.3g, which resulted in a final recovery of water, R_W = 20.1%.

It is interesting to note that around half of the M_W (R_W = 9.9%) were produced during the initial depressurization stage, which suggested that the aqueous-rich environment (S_A = 57.6%) promoted significantly the flow of aqueous phase under the combination of pressure reduction and high relative permeability [15]. The production of V_G, however, depends strongly on the rate of MH dissociation because there is limited free gas in the system. Thus, the time for half of the MH mass to dissociate, $t_{50,H}$ based on the gas production profile is 8.0 hr. We will compare the production behavior between 1.0 L and 3.3 L reactor in the scaling analysis section.

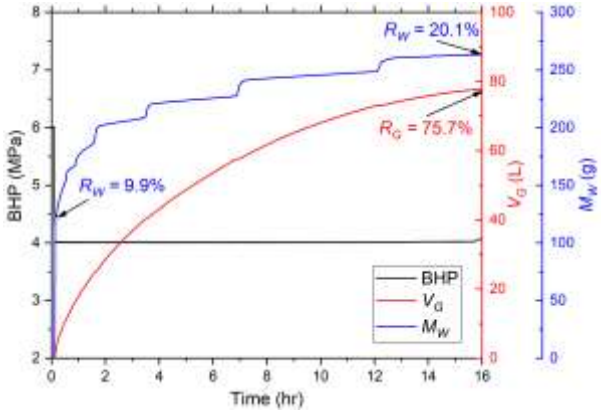

Fig. 5. Evolution of bottom-hole pressure, cumulative production of gas and water over time during dissociation.

3.3 Heat transfer characteristics

Fig. 6 shows the evolution of the spatial distribution of the T derived from the 21 thermocouple at different positions (see Fig. 2). It is noted that before the depressurization, a high temperature region is located at the upper section of the reactor, which can be attributed to the lower location of the cooling boundary and the imperfect insulation of the reactor. Upon depressurization, a low-T region (T = 4.0 °C) was observed near the bottom center of the reactor due to consumption of the sensible heat from the strong endothermic hydrate dissociation reaction (T_{eq} = 4.2 °C at P = 4.0 MPa). It can be deducted that S_H is the higher at the low-T region [16].

The low-T region shrank over time and based on the temperature gradient, it is obvious that the heat transfer direction is from the reactor outer boundary inward to the core center [17]. Such heat transfer characteristics is similar to that in the V = 1.0 L reactor with the only difference being the time needed for T to recover back. In the current 3.3 L reactor, it took more than 16 hrs; while it only took less than 5 hrs in the 1.0L reactor.

3.4 Scaling analysis

Comparing the production profiles between the 1.0L [10] and the 3.3 L reactor, we have identified some similarities. Table 2 lists the comparison of key parameters in MH formation and dissociation in the two different reactors. In terms of MH formation, to synthesize MHBS of the same saturation (S_H = 0.4 and S_A = 0.6), the mass of sand and the mole of gas and water should strictly adhere to the same ratio as the reactor volume, which is 0.30 in this study. In terms of the production behavior, we identified that increasing the MHBS sample volume resulted in an increase in R_G and a decrease in R_W. This is mainly attributed to the reduced production of M_W in the large reactor, which can be explained by the reduced capillary effect in the enlarged sample. In addition to the final amount of gas and water, we will conduct a dimensionless operation on the

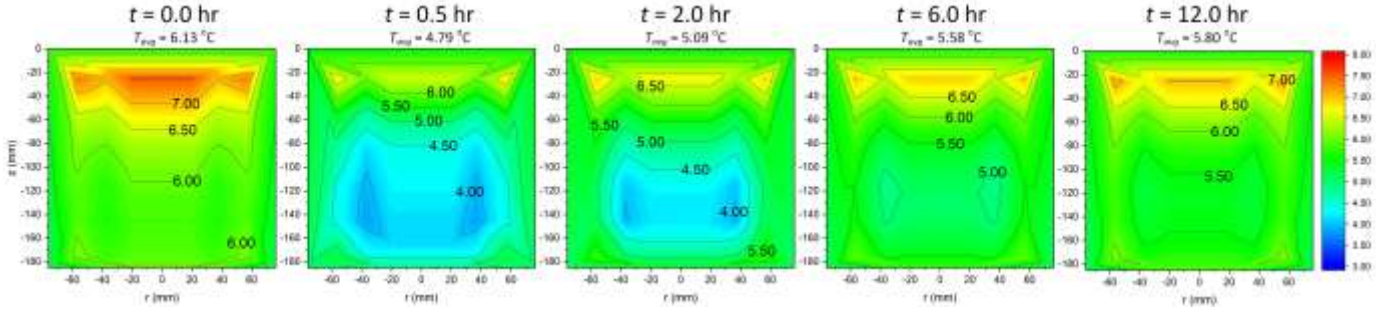

Fig 6. Evolution of spatial distribution of T over time during the MH dissociation in V = 3.3 L reactor.

governing equations to explain the similarly behavior observed in the gas production behavior in the full paper.

Table 2. Comparison of key parameters in MH formation and dissociation in two different reactors.

V = 1.0 L reactor		V = 3.3 L reactor		Ratio
$M_{sand,1}$	1480.5g	$M_{sand,2}$	4937.0g	0.30
V_{pore1}	421.3	V_{pore2}	1415.0	0.30
n_{G1}	1.45 mol	n_{G2}	4.75 mol	0.31
n_{A1}	414.0 g	n_{A2}	1308.5 g	0.32
R_{G1}	60.0%	R_{G2}	75.7%	0.79
R_{W1}	43.5%	R_{W2}	20.1%	2.16
$t_{50,H1}$	0.8 hr	$t_{50,H2}$	8.0 hr	0.10

4. SUMMARY AND CONCLUSION

To investigate the effect of scaling-up on the kinetic behavior of MH formation and dissociation, we have employed two reactors with different effect volumes of 1.0 L and 3.3 L to synthesize aqueous-rich MHBS and subject the samples to dissociation under the same BHP = 4.0 MPa. A detailed analysis on the response of P and T and the heat transfer characteristics were reported in this paper with a scaling analysis on the key parameters for MH formation and dissociation. We observe that increasing the MHBS sample size yielded an increase in the final recovery of gas and a decrease in the recovery of water. In addition, volume ratio should be strictly adhered to form MHBS of the same saturation. The results from this multi-scale experiments provide valuable information in experimental designs and possibly shed light to future field production tests in estimating the fluid production rate and volume.

ACKNOWLEDGEMENT

The financial support from the Lloyds Register Singapore (LRS) is greatly appreciated. Zhenyuan Yin appreciate the sponsorship from LRS and EDB for the IPP scholarship. Li Huang acknowledges the support from the China Scholarship Council for the sponsorship.

REFERENCE

[1] Boswell R, Collett TS. Current perspectives on gas hydrate resources. Energy & Environmental Science. 2011;4:1206-15.

[2] Yin Z, Chong ZR, Tan HK, Linga P. Review of gas hydrate dissociation kinetic models for energy recovery. Journal of Natural Gas Science and Engineering. 2016;35:1362-87.

[3] Li X-S, Xu C-G, Zhang Y, Ruan X-K, Li G, Wang Y. Investigation into gas production from natural gas hydrate: A review. Applied Energy. 2016;172:286-322.

[4] Moridis G, Collett TS, Pooladi-Darvish M, Hancock SH, Santamarina C, Boswell R, et al. Challenges, Uncertainties, and Issues Facing Gas Production From Gas-Hydrate Deposits. SPE-131792-PA. 2011;14:76-112.

[5] Yin Z, Linga P. Methane hydrates: A future clean energy resource. Chinese Journal of Chemical Engineering. 2019;https://doi.org/10.1016/j.cjche.2019.01.005.

[6] Yin Z, Moridis G, Tan HK, Linga P. Numerical analysis of experimental studies of methane hydrate formation in a sandy porous medium. Applied Energy. 2018;220:681-704.

[7] Song Y, Cheng C, Zhao J, Zhu Z, Liu W, Yang M, et al. Evaluation of gas production from methane hydrates using depressurization, thermal stimulation and combined methods. Applied Energy. 2015;145:265-77.

[8] Konno Y, Fujii T, Sato A, Akamine K, Naiki M, Masuda Y, et al. Key Findings of the World's First Offshore Methane Hydrate Production Test off the Coast of Japan: Toward Future Commercial Production. Energy & Fuels. 2017;31:2607-16.

[9] Wang Y, Feng J-C, Li X-S, Zhang Y. Experimental and modeling analyses of scaling criteria for methane hydrate dissociation in sediment by depressurization. Applied Energy. 2016;181:299-309.

[10] Chong ZR, Yin Z, Tan JHC, Linga P. Experimental investigations on energy recovery from water-saturated hydrate bearing sediments via depressurization approach. Applied Energy. 2017;204:1513-25.

[11] Li J-f, Ye J-l, Qin X-w, Qiu H-j, Wu N-y, Lu H-l, et al. The first offshore natural gas hydrate production test in South China Sea. China Geology. 2018;1:5-16.

[12] Yin Z, Moridis G, Chong ZR, Linga P. Effectiveness of multi-stage cooling processes in improving the CH4-hydrate saturation uniformity in sandy laboratory samples. Applied Energy. 2019;250:729-47.

[13] Peng D-Y, Robinson DBJI, Fundamentals EC. A new two-constant equation of state. 1976;15:59-64.

[14] Duan Z, Møller N, Greenberg J, Weare JH. The prediction of methane solubility in natural waters to high ionic strength from 0 to 250°C and from 0 to 1600 bar. Geochimica et Cosmochimica Acta. 1992;56:1451-60.

[15] Yang M, Fu Z, Zhao Y, Jiang L, Zhao J, Song Y. Effect of depressurization pressure on methane recovery from hydrate–gas–water bearing sediments. Fuel. 2016;166:419-26.

[16] Yin Z, Moridis G, Chong ZR, Tan HK, Linga P. Numerical Analysis of Experiments on Thermally Induced Dissociation of Methane Hydrates in Porous Media. Industrial & Engineering Chemistry Research. 2018;57:5776-91.

[17] Zhao J, Liu D, Yang M, Song Y. Analysis of heat transfer effects on gas production from methane hydrate by depressurization. International Journal of Heat and Mass Transfer. 2014;77:529-41.